Molecular BioSystems

RSC Publishing

PAPER

Proteomic and ionomic profiling reveals significant alterations of protein expression and calcium homeostasis in cystic fibrosis cells

Cite this: *Mol. BioSyst.*, 2013, **9**, 1117

Domenico Ciavardelli,*[ab] Melania D'Orazio,[c] Luisa Pieroni,[d] Ada Consalvo,[be] Claudia Rossi,[be] Paolo Sacchetta,[e] Carmine Di Ilio,[be] Andrea Battistoni[c] and Andrea Urbani[df]

Received 21st December 2012,
Accepted 4th April 2013

DOI: 10.1039/c3mb25594h

www.rsc.org/molecularbiosystems

Cystic fibrosis (CF) is an autosomal recessive disorder associated with mutations of the cystic fibrosis transmembrane conductance regulator (CFTR) gene and defective chloride transport across the epithelial cell membranes. Abnormal epithelial ion transport is the primary cause of persistent airway infections and chronic inflammation in CF patients. In order to gain further insight into the mechanisms of epithelial dysfunctions linked to CFTR mutations, we performed and integrated proteomic and ionomic analysis of human bronchial epithelial IB3-1 cells and compared them with a CFTR-complemented isogenic cell line (C38). Aside from changes that were consistent with known effects related to CFTR mutations, such as differences in glycolytic and gluconeogenic pathways and unfolded protein responses, differential proteomics highlighted significant alteration of protein expression and, in particular, of the 14-3-3 signalling pathway that is known to be involved in cellular calcium (Ca) homeostasis. Of note, restoring chloride efflux by acting on Ca cellular homeostasis has been shown to be a promising therapeutic intervention for CF. Ionomic analysis showed significant changes in the IB3-1 element profile compared with C38 cells and in particular we observed an increase of intracellular Ca that significantly correlates with intracellular zinc (Zn) levels, suggesting a synergistic role of Ca and Zn influx. This finding is particularly intriguing because Zn has been reported to be effective in CF treatment increasing Ca influx. Taken together, our proteomic and ionomic data reveal that CFTR mutation sets in motion endogenous mechanisms counteracting impaired chloride transport mainly acting on epithelial ion transport and increasing intracellular Ca, suggesting potential links between protein expression and this response.

Introduction

Cystic fibrosis (CF) is one of the most common life-shortening autosomal recessive inherited diseases characterized by defective chloride transport in epithelial cells and excess mucus secretion. It is caused by mutations in the cystic fibrosis transmembrane conductance regulator (CFTR) gene, resulting in defective cAMP-dependent chloride conductance.[1] The lack of a functional CFTR inhibits chloride (Cl^-) efflux from the cell, thus leading to an increase in intracellular sodium (Na^+). This alteration in intracellular ion concentration causes the production of a thick mucus layer, which reduces mucociliary clearance (MCC) of epithelial surfaces. This problem is particularly acute in the lung, which is typically subjected to chronic infections[2] that are the main cause of morbidity and mortality in CF. Several approaches have been proposed to counteract the ion transport defect. These include the reintroduction of the wild-type CFTR gene, the chemical correction or potentiation of mutant CFTR and the activation of Cl^- channels distinct from CFTR. In particular, the calcium-activated Cl^- channel (CaCC) and chloride channel protein 2 (ClC-2) may provide alternative Cl^- channels.[3,4] Of note, restoring the Cl^- efflux acting on calcium (Ca) homeostasis of epithelial cells has been shown to be a potential therapeutic approach.[5] In addition to the well

[a] *School of Engineering, Architecture, and Motor Science, "Kore" University of Enna, Cittadella Universitaria, Enna Bassa, 94100 Enna, Italy. E-mail: domenico.ciavardelli@unikore.it, d.ciavardelli@unich.it; Fax: +39 0871 541542; Tel: +39 0871 541587*
[b] *Center of Excellence on Aging (Ce.S.I.), Chieti, Italy*
[c] *Department of Biology, University of Rome Tor Vergata, Rome, Italy*
[d] *IRCCS S. Lucia, Rome, Italy*
[e] *Department of Experimental and Clinical Sciences, "G. d'Annunzio" University of Chieti-Pescara, Chieti, Italy*
[f] *Department of Internal Medicine, University of Rome Tor Vergata, Rome, Italy*

known defects in Cl^- and Na^+ transport, several studies have pointed out that in CF patients there are significant alterations in the homeostatic mechanisms controlling the intracellular and/or extracellular concentrations of iron, copper and zinc.[6–10]

In order to tentatively understand the complex interplay between the lack of CFTR secretion, ion channel regulation, and metal homeostasis, we have investigated the proteomic and ionomic profiles of IB3-1 cells compared to isogenic C38 cells. Proteomic analysis of IB3-1 cells using two-dimensional electrophoresis (2DE) and mass spectrometry (MS) has been previously described.[11] In fact, differential proteomics based on 2DE-MS has been recently proposed either to characterize protein expression in this CF cell model[12,13] or to tentatively explain the effects of potential therapeutic approaches.[14–16] Here, for the first time, we describe label-free LC-MS^E differential proteomic analysis of IB3-1 and C38 cells. This is a powerful approach which allows the identification and quantification of several hundreds of proteins. In fact, although 2DE-MS remains to be the preferred analytical approach to study post-translational protein modifications, LC-MS^E based proteomics is a high-throughput approach suitable for a wide description of complex biological systems based on peptide analysis instead of proteins. The high complementary potential of this approach to the 2DE protein analysis has been demonstrated in CF models.[17] Therefore, our study is expected to significantly integrate previous results obtained using 2DE-MS.

In contrast, aside from several studies focusing on the alterations between hydrogen carbonate (HCO_3^-), Cl^-, Na^+, and potassium (K^+) transports linked to CFTR dysfunction, the effect of CFTR mutation and impaired Cl^- efflux on trace element homeostasis using element profiling of CF epithelial cells has not yet been reported. Therefore, the goal of the here reported study is to tentatively assess the relationships between protein and ion dyshomeostasis linked to the absence of a functional CFTR channel.

This integrative approach indicates that increased calcium influx may be an endogenous mechanism adopted by IB3-1 cells in response to impaired Cl^- efflux and suggests a potential role of specific protein expression pathways in this self-response.

Experimental

Chemicals and reagents

Nitric acid (69%) and yttrium stock solution (Y, 10 mg L^{-1}, 1% HNO_3) were purchased from Fluka (Shnelldorf, Germany) and Romil (Cambridge, UK), respectively. A multi-element calibration standard stock solution (Mg, Al, K, Ca, Mn, Fe, Cu, Zn, Rb, 10 mg L^{-1}, 2% HNO_3) and a tuning solution (Li, Y, Ce, Tl, 10 mg L^{-1}, 2% HNO_3) were purchased from Agilent Technologies (Tokyo, Japan). Stock solutions and samples were diluted with deionised water with a specific resistance of 18.2 MΩ cm (Milli-Q system, Millipore, Watford, Hertfordshire, UK). Acetic acid, acetonitrile, anhydrous magnesium sulfate ($MgSO_4$), citric acid, dipotassium hydrogen phosphate (K_2HPO_4), ammonium sodium hydrogen phosphate ($NaNH_4HPO_4{\cdot}4H_2O$), glucose, urea, tris(hydroxymethyl) aminomethane (Tris), iodoacetamide (IAA), dithiothreitol (DTT), and [Glu1]-fibrinopeptide B were purchased from Sigma Aldrich (Shnelldorf, Germany). Sequence grade trypsin was purchased from Promega (Madison, WI, USA).

Cell culture

IB3-1 cells (ATCC CRL-2777) are transformed bronchial epithelial cells isolated from a pediatric CF patient who harbored the ΔF508/W1282X mutations within the CFTR gene, and were used in conjunction with the C38 cell line (ATCC CRL-2779), which was generated from IB3-1 by transfection with an adeno-associated viral vector encoding a full-length, wild-type CFTR adeno-associated viral cystic fibrosis transmembrane conductance regulator (AAVCFTR). Cell lines were obtained from the American Type Culture Collection (ATTC). Cells were routinely maintained at 37 °C in Dulbecco's modified Eagle's medium (D-MEM) (Euroclone) supplemented with 2 mM glutamine, 100 U mL^{-1} penicillin, 0.1 mg mL^{-1} streptomycin, and 10% heat-inactivated fetal calf serum (FCS), in a 5% CO_2 atmosphere. The flask coating procedure was carried out with 0.03 mg mL^{-1} collagen type I bovine, 0.01 mg mL^{-1} human fibronectin, and 0.1 mg mL^{-1} bovine serum albumin, dissolved in LHC basal medium.

To prepare samples for ionomic and proteomic analyses, 24 hours after seeding, the above described medium was substituted by a medium supplemented with 2% FCS and cells were incubated for further 48 hours. Then, the confluent, adherent monolayers were washed twice in sterile phosphate buffered solution (PBS), released from the plastic surface by treatment with trypsin–EDTA and finally collected by centrifugation at 700×*g*.

ICP-MS analysis

ICP-MS analysis of cells was performed as previously described.[18] Cell pellets were freeze dried using a Modulyo freeze-dryer (Thermo Savant, USA), and accurately weighted using an AX26 Delta Range balance (Mettler-Toledo, Greifensee, Switzerland). Acidic digestion of cell pellets was performed in sterile polystyrene tubes (15 mL, BD Falcon, BD Biosciences, Franklin Lakes, NJ) by adding 0.050 mL of 65% HNO_3/30% H_2O_2 = 4/1 and heating at 70 °C for 5 h. The digested samples were diluted to a final volume of 2.000 mL with 18 MO cm water and analysed using Inductively Coupled Plasma Mass Spectrometry (ICP-MS). The dilution factor was 200 for the analysis of Mg and K. The external standard method was applied for quantification. The HNO_3 concentration of external standard solutions was accurately matched to the final concentration of HNO_3 in the cell samples (*i.e.* 1.3%). The starting cell media and the supernatants were diluted 20 or 200 fold with 1.3% HNO_3 and analyzed by applying the standard addition method. The diluted samples were spiked at three concentration levels (1, 10 and 100 ng mL^{-1}). ^{89}Y (50 ng mL^{-1}) was used as an internal standard in both cases. ICP-MS analyses were performed using a 7500A ICP quadrupolar mass spectrometer (Agilent Technologies, Palo Alto, CA) fitted with an ASX-510 autosampler (CETAC, Omaha, NE, USA) and a peristaltic pump. A Babington nebulizer with a Scott spray chamber (Agilent Technologies) was used for sample introduction.

The following normal plasma conditions were applied: forward power = 1240 W; plasma gas flow rate = 15 L min^{-1}; carrier gas flow rate = 1.07 L min^{-1}; spray chamber temperature = 21 °C; sampler and skimmer cone: Ni, 1 and 0.4 mm inside diameter, respectively; sample uptake rate = 0.4 mL min^{-1}; sample depth = 8.8 mm; sampling period per mass = 0.3 s. The operating conditions were optimized for sensitivity using a 1×10^{-5} mg mL^{-1} solution of ^{7}Li, ^{89}Y and ^{205}Tl.[19,20] External calibration was performed for each element by analysing standard solutions obtained at different concentration levels by diluting the multi-element stock solution (Agilent Technologies). The internal standard solution was added on line to the samples by a T-piece giving a 20-fold dilution of the original concentrations of the internal standard element. Three replicate measurements were performed for each sample. Washing of the sample introduction system was performed with 1.3% HNO_3. Data analysis was performed using ChemStation software (Agilent Technologies).

Fluorimetric determination of intracellular calcium

C38 and IB3-1 cells grown to confluence on 10 cm coated-dishes were trypsinized, resuspended in culture medium at a density of 10^6 mL^{-1}, and loaded with the 2 μM fura-2 penta-acetoxymethyl (AM) ester (Molecular Probes, Eugene, Oregon, USA) for 30 min at 25 °C in the dark. Cells were subsequently washed with Ca^{2+}-containing buffer (140 mM NaCl, 5 mM KCl, 1 mM $MgCl_2$, 2 mM $CaCl_2$, 10 mM HEPES, and 5 mM glucose; pH 7.4) twice, resuspended in 0.1 mL of Ca^{2+}-containing buffer and incubated for further 15 min at 25 °C in the dark (to allow for de-esterification of the Fura-2/AM). Fura-2 fluorescence measurements were performed using a Perkin-Elmer LS 50B spectrofluorimeter (25 °C), immediately after 0.1 mL cell suspension was added to 0.9 mL of Ca^{2+}-containing buffer or Ca^{2+}-free buffer (140 mM NaCl, 5 mM KCl, 3 mM $MgCl_2$, 0.3 mM EGTA, 10 mM HEPES, and 5 mM glucose; pH 7.4) by measuring excitation signals at 340 nm and 380 nm and the emission signal at 510 nm. For calibration of intracellular Ca^{2+} ($[Ca^{2+}]_i$), the detergent Triton X-100 (0.1%) and $CaCl_2$ (5 mM) were added to the cuvette to obtain the maximal fura-2 fluorescence (R_{max}). The Ca^{2+} chelator EGTA (10 mM) was added to the cuvette to chelate Ca^{2+} and obtain the minimal fura-2 fluorescence (R_{min}). $[Ca^{2+}]_i$ was calculated as previously described,[21] assuming the apparent dissociation constant for fura-2 as 224 mM.

Label free proteomic analysis using LC-MS^E

Label-free quantitative proteomics was performed as previously described.[17,22,23] Briefly, cells were lysed in 100 mM Tris pH 7.5 containing 6 M urea. After centrifugation protein concentrations were determined in each supernatant and 100 μg of total protein per cell type was subject to trypsin digestion as previously described. After digestion, 0.270 μg μL^{-1} of triptic peptide solution containing 100 fmol μL^{-1} of Yeast Enolase digestion (SwissProt P00924) (Waters, Milford, MA, USA) added as an internal standard was used for shotgun proteomic analysis by means of Ultra Performance Liquid Chromatography on a nano ACQUITY UPLC System (Waters), coupled to a hybrid Quadrupole orthogonal acceleration Time-of-flight Mass Spectrometer (Q-Tof Premier, Waters Corp.). Mass spectrometry data were acquired in MS^E mode (Expression mode: data independent parallel parent and fragment ion analysis).

Continuum LC-MS data from four replicate experiments for each cell type were processed for qualitative and quantitative analysis using the software ProteinLynx Global Server v. 2.3 (PLGS, Waters). The qualitative identification of proteins was obtained by searching in a human database (UniProt KB/Swiss-Prot Protein Knowledgebase release 2011_06, of 31-May-11 containing 529 056 sequence entries, taxonomical restrictions: Homo Sapiens, 20 235 frequencies) to which data from *Saccharomyces cerevisiae* Enolase were appended. Identified proteins were normalized against P00924 entry (Enolase *S. cerevisiae*) in the quantitative analysis.[17,22]

Gene ontology and pathway analysis

Functional classification based on gene ontology (GO) terms related to biological processes and function, respectively, was performed using the web resource the Generic Gene Ontology Term Finder available at http//go.princeton.edu/cgi-bin/GOTerm Finder.[24] The GO Term Finder attempts to determine whether an observed level of annotation for a group of genes is significant within the context of annotation for all genes within the genome. Over-represented GO terms were identified.

Protein connectivity of differentially expressed proteins identified in LC-MS^E experiments were analyzed through the use of Ingenuity Pathways Analysis-IPA (Ingenuity® Systems, version 9.0, released date 2011-08-20, Content version: 3210, release date: 2011-05-17, http://www.ingenuity.com).

Statistical analysis

Significance of the differences in element concentrations between the two cell lines was assessed by the Mann–Whitney U test. Two factor ANOVA followed by the Fisher LSD post-hoc test was performed in order to assess the significance of differences in cytosolic $[Ca^{2+}]_i$ determined using fluorimetric analysis. The cell line and the experimental Ca^{2+} concentration were the independent factors. Spearman correlation analysis was performed in order to evaluate significant correlations between elements in each cell line. p values lower than 0.050 were considered statistically significant. Statistical analysis was performed with Statistica 6.0 (StatSoft Inc., Tulsa, OK), XLStat2007.1 (Microsoft, USA), and Microsoft Excel software.

Results and discussion

Alterations of protein expression in CF bronchial epithelial cells using label-free proteomics

In this study we performed differential protein expression analysis of IB3-1 and C38 cells and identified a mean ± standard deviation (SD) of 120 ± 4 and 139 ± 7 proteins in the four replicate experiments of IB3-1 and C38 cell extracts, respectively. Between them, we identified 11 and 16 down and up-regulated proteins, respectively, in IB3-1 cells compared with C38 cells (Table 1). Table 2 shows the results of GO analysis performed on differentially expressed proteins based on terms related to

Table 1 Differentially expressed proteins in ΔF508 CFTR human bronchial epithelial cells (IB3-1) compared with CFTR complemented isogenic cells (C38)

Accession[a]	GN[a] (IPA) symbol	Protein name	PLGS[b] score	IB3-1 : C38 $\log_e$ ratio[c]	IB3-1 : C38 $\log_e$ SD[d]	Location[e]	Type
P40926	MDH2	Malate dehydrogenase, mitochondrial	309	C38[f]	NC[g]	Cytoplasm	Enzyme
P04792	HSPB1	Heat shock protein beta-1	244	C38[f]	NC[g]	Cytoplasm	Other
P07910	HNRNPC	Heterogeneous nuclear ribonucleoproteins C1/C2	211	C38[f]	NC[g]	Nucleus	Other
P52272	HNRNPM	Heterogeneous nuclear ribonucleoprotein M	449	C38[f]	NC[g]	Nucleus	Other
P51991	HNRNPA3	Heterogeneous nuclear ribonucleoprotein A3	250	C38[f]	NC[g]	Nucleus	Other
Q3ZCM7	TUBB8	Tubulin beta-8 chain	607	−1.2	0.2	Unknown	Other
Q99867	TUBB4Q/n.a.	Putative tubulin beta-4q chain	556	−1.1	0.3	n.a.	n.a.
Q13509	TUBB3	Tubulin beta-3 chain	1540	−0.8	0.1	Cytoplasm	Other
Q9Y281	CFL2	Cofilin-2	385	−0.4	0.2	Unknown	Other
P09651	HNRNPA1	Heterogeneous nuclear ribonucleoprotein A1	480	−0.4	0.1	Nucleus	Other
P16949	STMN1	Stathmin	314	−0.3	0.2	Cytoplasm	Enzyme
P07900	HSP90AA1	Heat shock protein HSP 90-alpha	710	0.31	0.08	Cytoplasm	Enzyme
P14618	PKM2/PKM	Pyruvate kinase isozymes M1/M2	924	0.36	0.08	Unknown	Kinase
P12814	ACTN1	Alpha-actinin-1	770	0.4	0.1	Cytoplasm	Other
P07355	ANXA2	Annexin A2	1562	0.39	0.07	Plasma membrane	Other
Q9BUF5	TUBB6	Tubulin beta-6 chain	567	0.4	0.2	Cytoplasm	Other
P63104	YWHAZ	14-3-3 Protein zeta/delta	443	0.4	0.1	Cytoplasm	Enzyme
P62258	YWHAE	14-3-3 Protein epsilon	362	0.5	0.1	Cytoplasm	Other
P09382	LGALS1	Galectin-1	210	0.5	0.1	Extracellular space	Other
P35579	MYH9	Myosin, heavy chain 9, non-muscle	1532	0.5	0.1	Cytoplasm	Transporter
P17661	DES	Desmin	436	0.5	0.1	Cytoplasm	Transporter
P68104	EEF1A1	Eukaryotic translation elongation factor 1-alpha 1	745	0.5	0.1	Cytoplasm	Translation regulator
P00338	LDHA	L-Lactate dehydrogenase A chain	567	0.6	0.1	Cytoplasm	Enzyme
Q5VTE0	EEF1A1P5/ n.d.	Putative elongation factor 1-alpha-like 3	728	0.6	0.1	n.a.[f]	n.a.[f]
P08670	VIM	Vimentin	1926	0.60	0.07	Cytoplasm	Other
P07195	LDHB	L-Lactate dehydrogenase B chain	303	0.6	0.2	Cytoplasm	Enzyme
Q08043	ACTN3	Alpha-actinin-3	512	IB3-1[g]	NC[h]	Cytoplasm	Other

[a] Unique protein sequence identifier (accession) and gene name (GN) according to the UniProtKB/Swiss-Prot Protein Knowledgebase, release 2011_07 _June 28, 2011. [b] Protein Lynx Global Server score. [c] Expression ratio between IB3-1 and C38 cells. [d] Standard deviation. [e] According to IPA annotation. [f] Not annotated in IPA. [g] Protein found highly represented in IB3-1 cells. [h] Not calculated.

biological processes and functions, respectively. The down-regulated proteins were mainly related to nucleic acid binding and RNA processing. In particular, the heterogeneous nuclear ribonucleoproteins A3 (HNRNPA3), A1 (HNRPA1), C (HNRNPC), and M (HNRNPM) and the 27 kDa heat shock chaperone protein 1 (HSPB1) are significantly related to the spliceosome process of RNA (data not shown). Furthermore, we found that cytoskeletal and chaperone proteins were over-represented within the up-regulated proteins. Overall, these data suggest that cytoskeleton rearrangement and chaperone function as well as spliceosome activity were altered in CFTR mutant cells compared to wild type and are in agreement with previously published data.[11,25]

It should be noted that both the IB3-1 and the C38 cell lines express the ΔF508 mutant CFTR variant. Due to misfolding problems, this mutant protein is mainly retained in the ER as a core-glycosylated intermediate. Quality control in ER has a key role in the correct translocation and cellular localization of the native protein[26] in a process that requires molecular chaperones.[27] Our data showing overexpression of chaperones in the IB3-1 cell line compared to CFTR-complemented C38 suggest that this difference should not be related to this specific mutation, but, rather, to defects correlated with altered ion homeostasis due to the lack of CFTR. On the other hand, the presence of wild type CFTR on the plasma membrane influences the cytoskeletal organizational state[28] in line with the here reported observations.

It is also interesting to note that IB3-1 cells exhibit an altered expression of key enzymes of glucose metabolism such as mitochondrial malate dehydrogenase (MDH2), pyruvate kinase M2 (PKM2), and lactate dehydrogenase A (LDHA) and B (LDHB). These results are in agreement with a recently published study that shows a significant alteration of glucose metabolism in airway epithelial cells obtained from CF patients and decreased intracellular levels of glucose and glucose metabolites.[29] Furthermore, the increased expression levels of PKM2, LDHA, and LDHB suggest that glycolysis is the preferred pathway of glucose degradation in IB3-1 cells. This is a common signature of proliferating cells known as the Warburg effect that finally minimizes oxidative stress in cells.[30] Oxidative stress has been found to be increased in CF cells[31] inducing cell damage and apoptosis. Therefore, increased anaerobic glycolysis may indicate a potential anti-oxidant defence mechanism.[32]

Connectivity network analysis using IPA results in two overlapping networks (score = 63 and 13, respectively), which are related to genetic disorders, neurological diseases, and skeletal and muscular disorders as well as to cell death and cell growth and proliferation, respectively (Fig. 1A). According to the GO

Table 2 Gene ontology (GO) analysis of down- and up-regulated proteins in IB3-1 cells. GO analysis was performed using the biological process and functions of the ontology and the human gene ontology annotation (GOA) gene associations file. The cluster frequency calculated from the number of proteins annotated to the specific GO term and the total number of differentially expressed proteins, the frequency in the entire genome of all genes annotated to a specific GO, and the statistical significances of annotations of the list of genes to GO terms are shown

Gene ontology term	Cluster frequency	Genome frequency	Corrected, p-value[a]	Genes annotated to the term
Down-regulated proteins				
Biological process				
mRNA metabolic process	5 of 13 genes, 38.5%	690 of 46 279 genes, 1.5%	0.0001	P07910, P09651, P52272, P51991, P04792
Biological functions				
Nucleotide binding	8 of 13 genes, 61.5%	6896 of 46 279 genes, 14.9%	0.004	Q3ZCM7, P07910, P09651, P15531, P52272, P40926, P51991, Q13509
Up-regulated proteins				
Biological processes				
Cellular component organization at cellular level	11 of 17 genes, 64.7%	4578 of 46 279 genes, 9.9%	2×10^{-5}	P12814, Q08043, P17661, P08670, P35579, P09382, P07355, P07900, Q9BUF5, P63104, A6NMY6
Cell death	7 of 17 genes, 41.2%	2416 of 46 279 genes, 5.2%	0.003	P12814, Q08043, P08670, P09382, P62258, P63104, P14618
Glycolysis	3 of 17 genes, 17.6%	164 of 46 279 genes, 0.4%	0.007	P00338, P14618, P07195
Biological functions				
Protein binding	14 of 17 genes, 82.4%	9537 of 46 279 genes, 20.6%	5×10^{-6}	P12814, Q08043, P68104, P17661, P08670, P35579, P09382, P07355, P62258, P07900, P14618, P63104, P07195, A6NMY6

[a] Bonferroni corrected p values.

analysis, pyruvate metabolism and glycolysis–gluconeogenesis were significantly over-represented canonical pathways among the differential proteins (Fig. 1B). Furthermore, differential protein expression results in pathways linked to gap junction functionality and inflammatory response and the 14-3-3 mediated signalling pathway which is the most significant pathway identified ($p = 1.95 \times 10^{-9}$) (Fig. 1B). This canonical pathway has been related to neurodegenerative disorders, such as Alzheimer's disease.[33] In particular 14-3-3ζ, found to be up-regulated in IB3-1 cells, has been found to be neuroprotective against endoplasmic reticulum (ER) stress.[34]

However, 14-3-3 proteins are also involved in many other physiopathological conditions. In fact, 14-3-3 proteins are ubiquitous proteins that have a wide range of functions and are key regulators of protein assembly, trafficking and function.[35] Furthermore, 14-3-3 proteins are strictly involved in trafficking of ΔF508-CFTR[19] and ion channel regulation. In particular, 14-3-3ε proteins are known to modulate calcium-mediated Cl^- transport by interacting with several Ca^{2+} channels.[36,37] This function makes 14-3-3 proteins a particularly interesting candidate for research in the CF field. Both increased epithelial reabsorption of sodium and raised $[Ca^{2+}]_i$ have been implicated in the pathogenesis of cystic fibrosis. Furthermore, increased Ca^{2+} influx through the activated transient receptor potential canonical channel 6 (TRPC6) in IB3-1 cells has been recently reported.[38] However, the physiological role of the increase of Ca influx is still controversial. In fact, the increase of Ca^{2+} influx may activate Ca^{2+}-activated ion channels expressed in pulmonary epithelia such as CaCC.[3] Increased CaCC activity may partially compensate for the defective CFTR function in CF cells resulting in an alternative pathway of chloride transport in airway epithelial cells. For these reasons, the role of Ca^{2+}-activated ion transport has recently gained great attention in the treatment of CF.[39]

The downstream effect analysis performed using IPA, that results in biological functions predicted to be significantly activated or inhibited on the basis of differential protein profiles, suggests that the over-expression of galectin 1 and 14-3-3ε could result in increased intracellular levels of metals and $[Ca^{2+}]_i$ in IB3-1 cells (z score = 1.075, $p = 1.7 \times 10^{-2}$) (Fig. 1C). Although 14-3-3ε inhibits CaCC through a calmodulin-modulated pathway[36] thus inhibiting Cl^- secretion, this protein also inhibits the activity of the ubiquitous plasma membrane Ca^{2+} ATP-ase 1 (PMCA1) increasing $[Ca^{2+}]_i$.[37] Furthermore, increased expression levels of 14-3-3ε protein have been associated with increased $[Ca^{2+}]_i$ in stimulated HeLa cells.[40] However, it is still unclear how 14-3-3ε over-expression may affect $[Ca^{2+}]_i$ in unstimulated cells.

On the other hand, it has been shown that dimeric galectin 1 rapidly increases cytosolic $[Ca^{2+}]_i$ in neutrophils.[41]

Overall, these findings may indicate compensatory mechanisms used by IB3-1 cells to counteract the impaired Cl^- efflux, which result in increased $[Ca^{2+}]_i$.

ICP-MS analysis of IB3-1 cells reveals altered intracellular calcium levels

In order to verify the above mentioned hypothesis on the possible relationships between the differential protein expression pathways and variation in intracellular concentration of metals, we performed an ICP-MS analysis of IB3-1 and C38 cells. Given its multi-element capability, this approach allowed us to assess the effects of CFTR mutation on either $[Ca^{2+}]_i$ or other cellular elements. Element concentrations measured in C38 and IB3-1 cells are shown in Table 3 and Fig. 2.

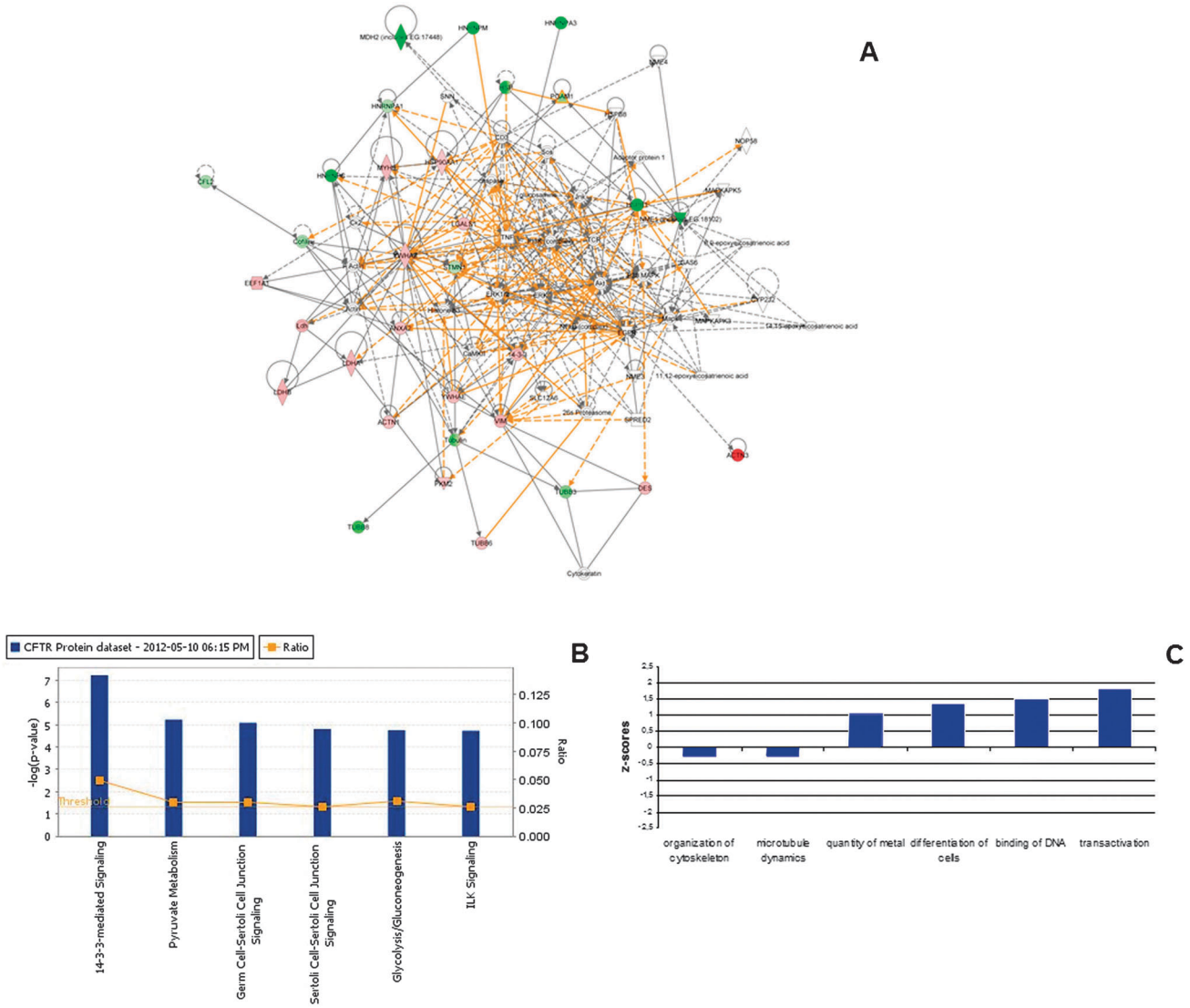

Fig. 1 Protein connectivity analysis using IPA. (A) Overlapping protein networks. Down- and up-regulated proteins in IB3-1 compared to C38 cells are shown in green and red, respectively. (B) Canonical pathways over-represented among the differentially expressed proteins. (C) *z*-scores associated with biological functions predicted to be significantly activated or inhibited in the IB3-1 cells compared to C38 cells on the basis of the differential protein expression. Abbreviations: ACTN1: alpha-actinin 1; ACTN3: actinin 3 alpha; Akt: protein kinase B; ANXA2: annexin A2; ANXA2P2: annexin A2 pseudogene 2; AR: androgen receptor; CaMKII: Ca^{2+}/calmodulin-dependent protein kinase II; CEBPB (includes EG:1051): Ccaat/enhancer binding protein beta; CFL2: cofilin 2 (muscle); Ck2: casein kinase 2; CYP2J2: cytochrome P450, family 2, subfamily J, polypeptide 2; DAXX: death-domain associated protein; DES: desmin; EEF1A1: eukaryotic translation elongation factor 1 alpha 1; EGFR: epidermal growth factor receptor; ERK: p42/44 map-kinase; FOS: FBJ murine osteosarcoma viral oncogene homolog; FUBP1: far upstream element (FUSE) binding protein 1; GAS6: growth arrest-specific 6; GLIS2: GLIS family zinc finger 2; HIF1A: hypoxia inducible factor 1, alpha subunit; Hmgb1: high mobility group box 1; HNRNPA1: heterogeneous nuclear ribonucleoprotein; HNRNPA3: heterogeneous nuclear ribonucleoprotein A3; HNRNPC: heterogeneous nuclear ribonucleoprotein C (C1/C2); HNRNPM: heterogeneous nuclear ribonucleoprotein M; HR: hairless homolog (mouse); HSF4: heat shock transcription factor 4; HSP: heat shock protein; HSP90AA1: heat shock protein 90 kDa alpha (cytosolic); HSPB1: heat shock 27 kDa protein 1; HSPB8: heat shock 22 kDa protein 8; Jnk: JUN kinase; Ldh: lactate dehydrogenase; LDHA: lactate dehydrogenase A; LDHB: lactate dehydrogenase B; LGALS1: soluble 1 lectin, galactoside-binding; Mapk: MAP kinase; MAPKAPK3: mitogen-activated protein kinase-activated protein kinase 3; MAPKAPK5: mitogen-activated protein kinase-activated protein kinase 5; MDH2: malate dehydrogenase 1 mitochondrial; MYC: v-myc myelocytomatosis viral oncogene homolog (avian); MYCBP: c-myc binding protein; MYCN: v-myc myelocytomatosis viral related oncogene; MYH9: myosin, heavy chain 9, non-muscle; NANOG: Nanog homeobox; NFkB: NF-KAPPA beta; NME1: nucleotide diphosphate kinase beta; NOP58: nucleolar protein 5, nucleolar protein NOP5/NOP58, SIK, Sik sp; NOP58: ribonucleoprotein homolog (yeast); P38 MAPK: P38 mitogen-activated protein kinase; PGAM1: phosphoglycerate mutase 1; PI3K (complex): 1-phosphatidylinositol 3-kinase; PKM2: pyruvate kinase M2; PLAGL1: pleiomorphic adenoma gene-like 1; PLAGL2: pleiomorphic adenoma gene-like 2; PPARGC1A: peroxisome proliferator-activating receptor gamma coactivator 1 alpha; SATB1: SATB homeobox 1; SLC12A6: solute carrier family 12 (potassium/chloride transporters), member 6; SMARCA2: SWI/SNF related, matrix associated, actin dependent regulator of chromatin, subfamily a, member 2; SNN: stannin; SOX12: sex determining region Y-box 12; SPRED2: sprouty-related, EVH1 domain containing 2; STMN1: stathmin 1; TCR: T-cell receptor; TEAD1: TEA domain family member 1; TEAD3: TEA domain family member 3; TEAD4: TEA domain family member 4; TFAM: transcription factor A, mitochondrial; TFE3: transcription factor binding to IGHM enhancer 3; TFEC: transcription factor EC; THRA: thyroid hormone receptor, alpha; THRB: thyroid hormone receptor, beta; TNF: tumor necrosis factor; TP53: tumor protein p53; TSG101: tumor susceptibility gene 101; TUBB3: tubulin, beta 3 class III; TUBB6: tubulin, beta 6 class V; TUBB8: tubulin, beta 8 class VIII; VIM: vimentin; YWHAE: 14-3-3 EPSILON; YWHAZ: 14-3-3-ZETA; YY1: YY1 transcription factor; ZEB2: zinc finger E-box binding homeobox 2; ZNF148: zinc finger protein 148.

Table 3 Element concentrations in C38 and IB3-1 cells. Cells were grown as described in Materials and methods section. Data are mean (SD) (ng mg^{-1}, dry weight)

Element (*m*/*z*)	C38 cells, mean (SD),[a] ng mg^{-1} (dry weight)	IB3-1 cells, mean (SD),[a] ng mg^{-1} (dry weight)
Mg (24)	1099 (119)	919 (140)
K (39)	29 410 (4198)	24 146 (1886)
Ca (43)	50 (13)	84 (12)
Mn (55)	2.5 (0.3)	2.5 (0.4)
Fe (57)	44 (16)	35 (14)
Co (59)	0.09 (0.01)	0.07 (0.02)
Cu (63)	4.3 (0.5)	5.8 (0.9)
Zn (66)	142 (15)	157 (14)
Rb (85)	17 (2)	5 (2)

[a] Standard deviation.

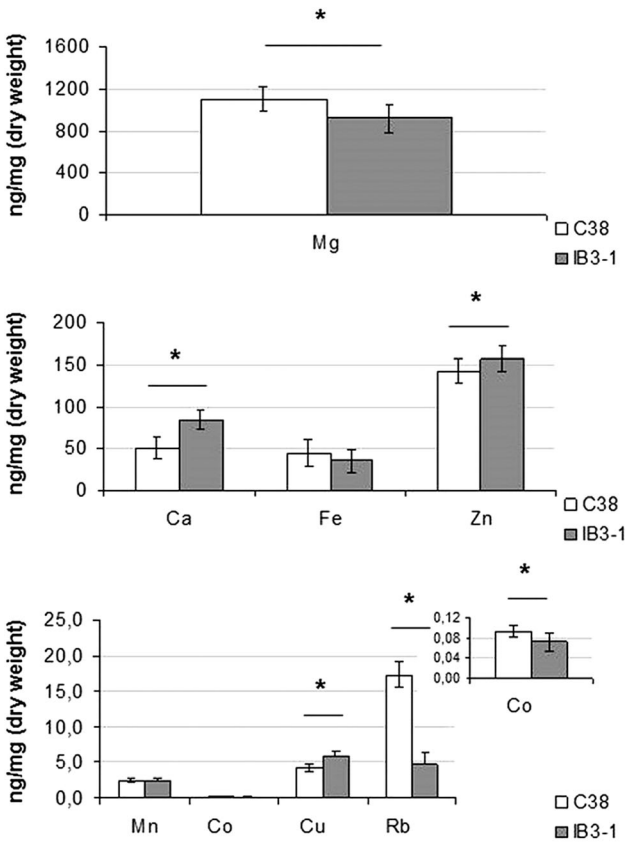

Fig. 2 Element profiles of IB3-1 and C38 cells. Data are mean concentrations (μg g^{-1}, dry weight). Bars represent the mean standard deviations. The asterisks indicate significant differences at the 95% confidence level.

We found decreased levels of magnesium (Mg; $p = 0.045$), K ($p = 0.036$), cobalt (Co; $p = 0.045$), and rubidium (Rb; $p = 0.003$) as well as increased levels of copper (Cu; $p = 0.004$) and zinc (Zn; $p = 0.023$) in IB3-1 cells. These findings demonstrate that the absence of a functional CFTR strongly affects element homeostasis in CF cells.

More importantly, we found that $[Ca^{2+}]_i$ significantly increased in IB3-1 cells ($p = 0.003$; Fig. 2) corroborating the idea that impaired Cl^- efflux induces some compensatory mechanisms that finally raise Ca^{2+} influx.

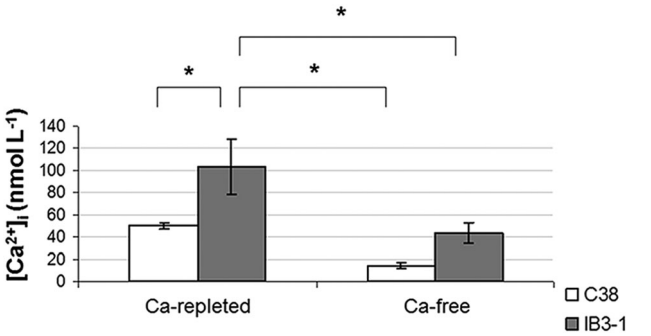

Fig. 3 Fluorimetric determination of intracellular Ca^{2+} in C38 and IB3-1 cells. Ca^{2+} concentration was determined either in Ca-repleted or Ca-free solutions. Data are mean concentrations (nmol L^{-1}). Bars represent the standard error of the mean (SEM) calculated as SEM = SD/$\sqrt{n}$, SD = standard deviation, $n = 3$. The asterisks indicate significant differences ($p < 0.050$).

This finding was further corroborated by fluorimetric determination of cytosolic $[Ca^{2+}]_i$ in living cells. According to ICP-MS data, IB3-1 cells showed increased $[Ca^{2+}]_i$ compared to C38 cells ($p = 0.025$, Fig. 3). A difference in $[Ca^{2+}]_i$ between IB3-1 and C38 cells was observed also upon shift of the cells in a Ca^{2+}-free buffer, although under this condition the difference in $[Ca^{2+}]_i$ does not reach a statistical significance ($p = 0.162$, Fig. 3). However, we observed that the decrease in $[Ca^{2+}]_i$ exhibited in the Ca-free buffer was more pronounced for IB3-1 cells ($p = 0.015$, Fig. 3) than in C38 cells ($p = 0.096$). These results suggest that the increase of $[Ca^{2+}]_i$ likely involves an enhancement in Ca^{2+} influx in IB3-1 cells, whereas the differences in calcium release from intracellular stores in these cell lines are likely to be negligible and reflect the initial differences in accumulation.

As discussed above, there is growing evidence that increased Ca^{2+}-mediated Cl^- efflux may be a viable treatment option for CF. Although further experiments are needed to better understand the role of up-regulation of galectin-1 and 14-3-3 proteins in this cellular adaptation process to counterbalance impaired chloride secretion, our data are in line with the prediction of down-stream effect analysis.

Spearman's correlation analysis shows that $[Ca^{2+}]_i$ is inversely correlated with Rb ($r = -0.709$; $p = 0.014$) and shows a trend toward inverse correlation with K ($r = -0.578$; $p = 0.103$). The increase of $[Ca^{2+}]_i$ has been related to increased K efflux in epithelial cells.[5] This finding was further corroborated by the simultaneous decrease of intracellular K and Rb. In fact, we have found a significant direct correlation between Rb and K ($r = 0.957$; $p = 0.043$). Notably, Rb has been often proposed as a tracer for K movement across the cell membrane.[42]

In contrast, it is significant that Ca directly correlates with intracellular Cu ($r = 0.856$, $p = 0.030$), and, in particular, with Zn levels ($r = 0.849$, $p = 0.032$, Fig. 4A) in IB3-1 cells. In contrast, we did not find these correlations for Cu ($r = -0.678$, $p = 0.093$) and Zn ($r = -0.178$, $p = 0.702$, Fig. 4B) in C38 cells. The regulation of Zn homeostasis in bronchial epithelial cell lines has been extensively investigated.[43] It is intriguing to speculate that the increase of $[Ca^{2+}]_i$ may be associated with increased ROS production and oxidative stress[44] followed by the activation of

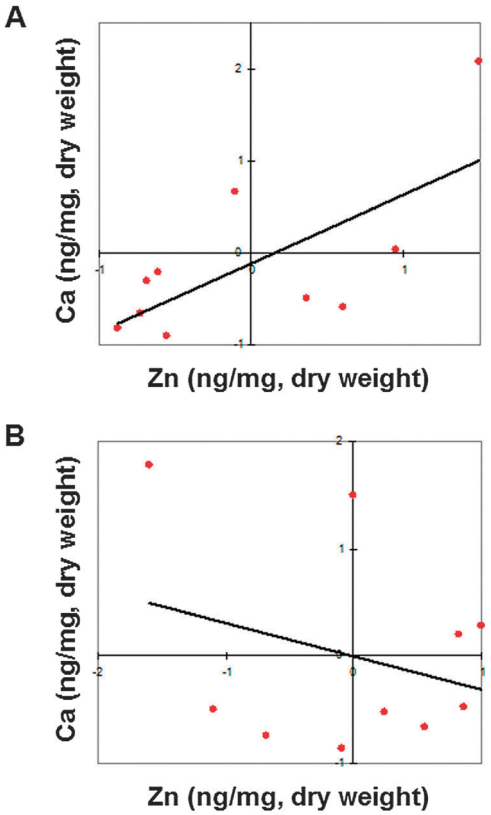

Fig. 4 Correlations between Ca^{2+} and Zn^{2+} in IB3-1 and C38 cells. (A) There is a significant direct correlation between intracellular Ca^{2+} and Zn^{2+} (r = 0.849, p = 0.032) in IB3-1 cells. (B) This relationship is not significant in C38 cells (r = −0.178, p = 0.702). Correlations were assessed using non-parametric Spearman's correlation analysis performed at the 95% confidence level.

an antioxidant response such as increased expression of the metallothioneins that has been reported in IB3-1 cells following treatments aimed at restoring CFTR function.[45] These Cu and Zn-binding proteins are strictly involved in Zn homeostasis and have been related to Zn absorption.[46] Here, we did not find metallothionein over-expression in IB3-1 cells. However, the up-regulation of metallothioneins in response to increased oxidative stress[30] could be related to the observed increases of intracellular Zn and Cu. Of note, as discussed above, both Zn and Cu levels are directly correlated with Ca levels in IB3-1 cells. Finally, it should be reminded that it is known that extracellular Zn^{2+} improves Ca^{2+} mediated Cl^- efflux by regulation of ATP-gated P2 purinergic ionotropic receptors (P2X).[47] Activation of P2X Ca^{2+} entry channels may have therapeutic benefit for CF independently of the CFTR genotype.[48] Our data show that Ca and Zn are strongly correlated in IB3-1 cells, suggesting that there could be a further Zn-activated mechanism resulting in increased $[Ca^{2+}]_i$.

Conclusion

In this study we show that the absence of CFTR results in significant alterations of proteomic and ionomic profiles in CF cells compared with an isogenic cell line expressing a functional CFTR transporter. Our findings suggest that IB3-1 cells activate endogenous mechanisms that finally increase $[Ca^{2+}]_i$. This response may potentially counteract impaired Cl^- efflux and is probably linked to the observed protein expression pathways. It is currently unclear how changes in protein expression levels may affect Ca homeostasis in CFTR cells and, therefore, the assessment of the mechanism underlying this adaptation response deserves further investigations.

Abbreviations

2DE	two-dimensional electrophoresis
Ca	calcium
CaCC	calcium-activated Cl^- channel
Ce	cerium
CF	cystic fibrosis (CF)
CFTR	cystic fibrosis transmembrane conductance regulator
Cl^-	chloride
ClC-2	chloride channel protein 2
Co	cobalt
Cu	copper
D-MEM	Dulbecco's modified Eagle's medium
DTT	dithiothreitol
ER	endoplasmic reticulum
FCS	fetal calf serum
Fe	iron
GN	gene name
GO	gene ontology
GOA	gene ontology annotation
HCO_3^-	hydrogen carbonate
HNO_3	nitric acid
IAA	iodoacetamide
ICP-MS	inductively coupled plasma mass spectrometry
IPA	ingenuity pathway analysis
K	potassium
K_2HPO_4	dipotassium hydrogen phosphate
LDHA	lactate dehydrogenase A
LDHB	lactate dehydrogenase B
Li	lithium
MCC	mucociliary clearance
MDH2	malate dehydrogenase
Mg	magnesium
$MgSO_4$	anhydrous magnesium sulfate
MS	mass spectrometry
Mn	manganese
Na^+	sodium
$NaNH_4HPO_4$	ammonium sodium hydrogen phosphate
Ni	nickel
P2X	P2 purinergic ionotropic receptors
PBS	phosphate buffered solution
PKM2	pyruvate kinase M2
PMCA1	plasma membrane Ca^{2+} ATP-ase 1
Q-Tof	quadrupole orthogonal acceleration time-of-flight
Rb	rubidium

SD	standard deviation
Tl	thallium
Tris	tri(hydroxymethyl) aminomethane
TRPC6	transient receptor potential canonical channel 6
UPLC	ultra performance liquid chromatography
Y	yttrium
Zn	zinc

Acknowledgements

This work was partially supported by the Italian Cystic Fibrosis Research Foundation (Grant FFC# 11/2008 to A.B.) with a contribution from Studio Palladio 2000, Sandrigo (VI). Thanks are due to Dr Blasco Morozzo della Rocca for his help in fluorimetric analyses of calcium concentration.

References

1 B. Kerem, J. M. Rommens, J. A. Buchanam, D. Markiewicz, T. K. Cox, A. Chakravarti, M. Buchwald and L. C. Tsui, *Science*, 1989, **245**(4922), 1073–1080.
2 M. T. Clunes and R. T. Boucher, *Drug Discovery Today: Dis. Mech.*, 2007, **4**(2), 63–72.
3 L. L. Clarke, B. R. Grubb, J. R. Yankaskas, C. U. Cotton, A. McKenzie and R. C. Boucher, *Proc. Natl. Acad. Sci. U. S. A.*, 1994, **91**(2), 479–483.
4 E. M. Schwiebert, L. P. Cid-Soto, D. Stafford, M. Carter, C. J. Blaisdell, P. L. Zeitlin, W. B. Guggino and G. R. Cutting, *Proc. Natl. Acad. Sci. U. S. A.*, 1998, **95**(7), 3879–3884.
5 A. Zsembery and D. Hargitai, *Wien. Med. Wochenschr.*, 2008, **158**, 562–564.
6 M. N. Pond, A. M. Morton and S. P. Conway, *Respir. Med.*, 1996, **90**(7), 409–413.
7 D. W. Reid, N. J. Withers, L. Francis, J. W. Wilson and T. C. Kotsimbos, *Chest*, 2002, **121**(1), 48–54.
8 S. S. Percival, G. P. A. Kauwell, E. Bowser and M. Wagner, *J. Am. Coll. Nutr.*, 1999, **18**(6), 614–619.
9 K. Best, K. McCoy, S. Gemma and R. A. Disilvestro, *Metabolism*, 2004, **53**(1), 37–41.
10 N. F. Krebs, M. Sontag, F. J. Accurso and K. M. Hambidge, *J. Pediatr.*, 1998, **133**(6), 761–764.
11 J. F. Collawn, L. Fu and Z. Bebok, *Expert Rev. Proteomics*, 2010, **7**(4), 495–506.
12 H. B. Pollard, O. Eidelman, C. Jozwik, W. Huang, M. Srivastava, X. D. Ji, B. McGowan, C. F. Norris, T. Todo, T. Darling, P. J. Mogayzel, P. L. Zeitlin, J. Wright, W. B. Guggino, E. Metcalf, W. J. Driscoll, G. Mueller, C. Paweletz and D. M. Jacobowitz, *Mol. Cell. Proteomics*, 2006, **5**(9), 1628–1637.
13 H. B. Pollard, X. D. Ji, C. Jozwik and D. M Jacobowitz, *Proteomics*, 2005, **5**(8), 2210–2226.
14 P. Gomes-Alves, S. Neves, A. V. Coelho and D. Penque, *J. Proteomics*, 2009, **73**(2), 218–230.
15 O. V. Singh, H. B. Pollard and P. L. Zeitlin, *Mol. Cell. Proteomics*, 2008, **7**(6), 1099–1110.
16 P. Gomes-Alves, F. Couto, C. Pesquita, A. V. Coelho and D. Penque, *Biochim. Biophys. Acta*, 2010, **1804**(4), 856–865.
17 L. Pieroni, F. Finamore, M. Ronci, D. Mattoscio, V. Marzano, S. L. Mortera, S. Quattrucci, G. Federici, M. Romano and A. Urbani, *Mol. BioSyst.*, 2011, **7**(3), 630–639.
18 D. Ciavardelli, S. Ammendola, M. Ronci, A. Consalvo, V. Marzano, M. Lipoma, P. Sacchetta, G. Federici, C. Di Ilio, A. Battistoni and A. Urbani, *Mol. BioSyst.*, 2011, **7**, 608–619.
19 D. Ciavardelli, A. Consalvo, V. Caldaralo, M. L. Di Vacri, S. Nisi, C. Corona, V. Frazzini, P. Sacchetta, A. Urbani, C. Di Ilio and S. L. Sensi, *Metallomics*, 2012, **4**(12), 1321–1332.
20 D. Ciavardelli, P. Sacchetta, G. Federici, C. Di Ilio and A. Urbani, *Talanta*, 2010, **80**, 1513–1525.
21 G. Grynkiewicz, M. Poenie and R. Y. Tsien, *J. Biol. Chem.*, 1985, **260**, 3440–3450.
22 V. Marzano, S. Santini, C. Rossi, M. Zucchelli, A. D'Alessandro, C. Marchetti, M. Mingardi, V. Stagni, D. Barilà and A. Urbani, *J. Proteomics*, 2012, **75**(15), 4632–4646.
23 S. D'Aguanno, I. D'Agnano, M. De Canio, C. Rossi, S. Bernardini, G. Federici and A. Urbani, *Mol BioSyst.*, 2012, **8**(4), 1068–1077.
24 E. I. Boyle, S. Weng, J. Gollub, H. Jin, D. Botstein, J. M. Cherry and G. Sherlock, *Bioinformatics*, 2004, **20**(18), 3710–3715.
25 M. Ollero, F. Brouillard and A. Edelman, *Proteomics*, 2006, **6**(14), 4084–4099.
26 L. Ellgaard and A. Helenius, *Nat. Rev. Mol. Cell Biol.*, 2003, **4**(3), 181–191.
27 M. D. Amaral, *J. Mol. Neurosci.*, 2004, **23**(1–2), 41–48.
28 S. Monterisi, M. Favia, L. Guerra, R. A. Cardone, D. Marzulli, S. J. Reshkin, V. Casavola and M. Zaccolo, *J. Cell Sci.*, 2012, **125**(Pt 5), 1106–1117.
29 D. R. Wetmore, E. Joseloff, J. Pilewski, D. P. Lee, K. A. Lawton, M. W. Mitchell, M. V. Milburn, J. A. Ryals and L. Guo, *J. Biol. Chem.*, 2010, **285**(40), 30516–30522.
30 M. G. Vander Heiden, L. C. Cantley and C. B. Thompson, *Science*, 2009, **324**(5930), 1029–1033.
31 M. Rottner, S. Tual-Chalot, H. A. Mostefai, R. Andriantsitohaina, J. M. Freyssinet and M. C. Martínez, *PLoS One*, 2011, **6**(9), e24880.
32 C. Ruckenstuhl, S. Büttner, D. Carmona-Gutierrez, T. Eisenberg, G. Kroemer, S. J. Sigrist, K. U. Fröhlich and F. Madeo, *PLoS One*, 2009, **4**(2), e4592.
33 M. K. Dougherty and D. K. Morrison, *J. Cell Sci.*, 2004, **117**, 1875–1884.
34 N. Murphy, H. P. Bonner, M. W. Ward, B. M. Murphy, J. H. Prehn and D. C. Henshall, *J. Neurochem.*, 2008, **106**(2), 978–988.
35 V. Obsilova, J. Silhan, E. Boura, J. Teisinger and T. Obsil, *Physiol. Res.*, 2008, **57**, S11–S21.
36 H. C. Chan, W. L. Wu, S. C. So, Y. W. Chung, L. L. Tsang, X. F. Wang, Y. C. Yan, S. C. Luk, S. S. Siu, S. K. Tsui, K. P. Fung, C. Y. Lee and M. M. Waye, *Biochem. Biophys. Res. Commun.*, 2000, **270**(2), 581–587.

37 C. I. Linde, F. Di Leva, T. Domi, S. C. Tosatto, M. Brini and E. Carafoli, *Cell Calcium*, 2008, **43**, 550–561.
38 F. Antigny, C. Norez, L. Dannhoffer, J. Bertrand, D. Raveau, P. Corbi, C. Jayle, F. Becq and C. Vandebrouck, *Am. J. Respir. Cell Mol. Biol.*, 2011, **44**, 83–90.
39 F. Ratjen, *Curr. Opin. Pulm. Med.*, 2007, **13**(6), 541–546.
40 A. Rimessi, L. Coletto, P. Pinton, R. Rizzuto, M. Brini and E. Carafoli, *J. Biol. Chem.*, 2005, **280**(44), 37195–37203.
41 S. Karmakar, R. D. Cummings and R. P. McEver, *J. Biol. Chem.*, 2005, **280**(31), 28623–28631.
42 M. G. McKay, R. W. Kirby and K. Lawson, *Methods Mol. Biol.*, 2008, **491**, 267–277.
43 P. D. Zalewski, A. Q. Truong-Tran, D. Grosser, L. Jayaram, C. Murgia and R. E. Ruffin, *Pharmacol. Ther.*, 2005, **150**(2), 127–149.
44 L. L. Dugan, S. L. Sensi, L. M. T. Canzoniero, S. D. Handran, S. M. Rothman, T. S. Lin, M. P. Goldberg and D. W. Choi, *J. Neurosci.*, 1995, **15**(10), 6377–6388.
45 J. M. Wright, P. L. Zeitlin, L. Cebotaru, S. E. Guggino and W. B. Guggino, *Physiol. Genomics*, 2004, **16**, 204–211.
46 P. Coyle, J. C. Philcox, L. C. Carey and A. M. Rofe, *Cell Mol. Life Sci.*, 2002, **59**, 627–647.
47 A. Zsembery, J. A. Fortenberry, L. Liang, Z. Bebok, T. A. Tucker, A. T. Boyce, G. M. Braunstein, E. Welty, P. D. Bell, E. J. Sorscher, J. P. Clancy and E. M. Schwiebert, *J. Biol. Chem.*, 2004, **270**, 10720–10729.
48 D. Hargitai, A. Pataki, G. Raffai, M. Füzi, T. Dankó, L. Csernoch, P. Várnai, G. P. Szigeti and A. Zsembery, *Respir. Physiol. Neurobiol.*, 2010, **170**(1), 67–75.

